



ELSEVIER

Contents lists available at ScienceDirect

Wear

journal homepage: [www.elsevier.com/locate/wear](http://www.elsevier.com/locate/wear)

# Reproducing automotive engine scuffing using a lubricated reciprocating contact

T.J. Kamps<sup>a,\*</sup>, J.C. Walker<sup>a</sup>, R.J. Wood<sup>a</sup>, P.M. Lee<sup>b</sup>, A.G. Plint<sup>c</sup>

<sup>a</sup> National Centre for Advanced Tribology at Southampton, Engineering and the Environment, University of Southampton, Highfield, Southampton SO17 1BJ, UK

<sup>b</sup> Tribology Evaluations and Analysis, Southwest Research Institute, P.O. Drawer 28510, San Antonio, TX 78238-0510, USA

<sup>c</sup> Phoenix Tribology Ltd, 29A Freemantle House, Kingsclere Park, Kingsclere RG20 4SW, UK

## ARTICLE INFO

### Article history:

Received 15 September 2014

Received in revised form

11 December 2014

Accepted 28 December 2014

Available online 6 January 2015

### Keywords:

Automotive

FIB

Grey cast iron

High speed friction

Lubrication

Scuffing

## ABSTRACT

The frequency and severity of scuffing in automotive engines has the potential to increase due to new low-viscosity lubricants for fuel efficiency and increased cylinder power output. This work is to understand the fundamental causes and events resulting in piston ring and liner scuffing. A TE-77 high frequency reciprocating tribometer was used with a synthetic PAO base oil (4cSt) to reciprocate a 52100 G5 barrel against a ground pearlitic Grade 250 grey cast iron.

Samples were run-in at 50 N and 10 Hz prior to a temperature ramp to 150 °C followed by a discreet load ramp to 1 kN (0.49 GPa). The tests were terminated when a sharp increase in the average friction force was observed indicating that scuffing had occurred. 3D optical profilometry showed that the scuffed cast iron surface consisted of smeared platelets and craters of 35 μm depth. SEM and EDX analyses suggested adhesive transfer of cast iron material to the counter-surface was occurring by failure along lamellar graphite interfaces. Tests were repeated using instantaneous high-speed friction data and indicated that micro-scuffing initiated at a load of 620 N. Focused ion beam cross-sections of the mildly scuffed surface confirmed the mechanism of sub-surface crack initiation occurring along lamellar graphite boundaries.

© 2015 Elsevier B.V. All rights reserved.

## 1. Introduction

The frequency and severity of scuffing in automotive engines has the potential to increase due to new low-viscosity lubricants for fuel efficiency and increased cylinder power output. A detailed understanding of the scuffing process would be valuable in controlling its initiation and progression. An immediate obstacle is that the literature is undecided on the scuffing definition as well as the mechanism that causes it [1–4]. Scuffing has been defined by the organisation for economic co-operation and development (OECD) as “local damage caused by the occurrence of solid-phase welding between sliding surfaces without local surface melting” [5] however many have discussed that scuffing is a complex evolution of the contact before this point [6–8]. Numerous theoretical qualitative and quantitative models for scuffing exist mostly based on calculations using temperature and pressure [9]. However, experimental investigations into scuffing initiation have

been limited due to the rapid progression to seizure in a matter of minutes [10].

Advances in predicting and detecting scuffing have been achieved by electrostatic sensors [11–13], acoustic emission sensors [14,15] and high speed friction data [16]. Electrostatic sensors can detect charging of a surface due to oil starvation, changes in oxidation states and also charged particles ejected from the contact during scuffing [17]. Electrostatic sensors have been used to detect different wear regimes in camshaft testing as well as first and second transitions scuffing for a lubricated reciprocating point contact [11,13]. Acoustic emission sensors can be used to measure transient elastic stress waves in a surface caused by plastic deformation during scuffing events. This has been used to indicate different levels of piston ring on liner scuffing damage in a reciprocating tribometer [15]. High speed friction data allows a change in friction force, indicating scuffing, to be mapped as a function of displacement. This has been used successfully to detect starting locations and propagation of heavy duty diesel fuel injector scuffing damage in a reciprocating tribometer [16]. The technique measured the difference between the instantaneous friction force at the onset of scuffing compared to the beginning of the test in order to determine failure initiation. This work is to understand the fundamental causes and events leading to piston

\* Corresponding author.

E-mail addresses: [T.Kamps@soton.ac.uk](mailto:T.Kamps@soton.ac.uk) (T.J. Kamps), [J.Walker@soton.ac.uk](mailto:J.Walker@soton.ac.uk) (J.C. Walker), [R.Wood@soton.ac.uk](mailto:R.Wood@soton.ac.uk) (R.J. Wood), [Peter.Lee@swri.org](mailto:Peter.Lee@swri.org) (P.M. Lee), [info@phoenix-tribology.com](mailto:info@phoenix-tribology.com) (A.G. Plint).

ring and liner scuffing using a TE-77 high frequency reciprocating tribometer equipped with high speed data acquisition.

Much of the published literature on scuffing uses a point contact [12,13,18] which, whilst successfully generates a scuffed surface, does not represent the pressure or geometry of a piston ring on cylinder liner contact. Typically the pressures found in the genuine contact are an order of magnitude lower than those that can be achieved using a point contact. The high pressures cause rapid deterioration of the original surface topography, resulting in the experiment running on the subsurface or significantly disturbed surface. This substantially affects the magnitude, progression and often the mode of scuffing wear that occurs. In the line contact, used in the work presented, the load was shared between many asperities, reducing the contact pressure. This allowed the contact load to be finely adjusted to investigate the evolution of the scuffing mechanism. Differentiation between different stages of scuffing was achieved by analysing high speed friction data during testing.

## 2. Experimental

The cylinder liner was simulated using a flat plate, 58 mm × 38 mm × 4 mm, of Grade 250 pearlitic flake graphite cast iron. The plate was surface ground at 45° to the reciprocating direction to achieve a bearing surface of at least 60%, which is similar to plateau honed liner surfaces in service [19]. The piston ring was simulated using a 6 mm diameter 52100 roller bearing element, 10 mm in length, with a G5 surface tolerance and 0.5 mm chamfer at each end.

The Grade 250 cast iron plate was sectioned in the transverse plane, mounted in Bakelite resin and polished to 1 μm diamond finish. The micro-structure was analysed using a BX51 Olympus optical microscope.

The hardness of both samples was measured using a Vickers hardness machine with an indentation load of 10 kgf. The surface topography of the samples was measured using a Taylor Hobson Talysurf diamond stylus: mild-scuffed cast iron data length 8 mm and  $l_c=0.8$  mm (cut off length); severe-scuffed cast iron data length 8 mm and  $l_c=2.5$  mm; roller bearing data length 4.1 mm and  $l_c=0.25$  mm.

Before both samples were tested in the tribometer they were cleaned using isopropanol in an ultrasonic bath. The tribometer was configured to reciprocate the roller bearing at 10 Hz over a stroke of 25 mm against the flat plate forming a line contact which was lubricated by a drip feed from one of the stroke reversal positions, Fig. 1a.

The lubricant used was a polyalphaolefin (PAO) with a viscosity of 4cSt at 100 °C. It was drip fed at 5 ml/h through a needle which was arranged such that the meniscus of the droplet formed on the end of the needle and was disrupted by the reciprocating cylinder, causing the PAO to be pulled via capillary forces into the contact interface.

At the start of the experiment the contact was run-in by reciprocating the roller bearing for 30 min at 20 °C and 50 N. Following run-in the temperature was increased at a rate of 4.3 °C/min from 20 °C to 150 °C to simulate engine operating temperatures. To allow the samples to reach thermal equilibrium the experiment was held for 30 min at 150 °C. The load was then increased from 50 N (0.11 GPa) to 1 kN (0.49 GPa) at a rate of 31.6 N/min until severe-scuffing occurred, Fig. 1b.

A rapid rise in average friction force was used as an indicator to determine whether severe-scuffing was occurring. This technique was chosen as it has been frequently reported in the literature [18,20–23]. The time averaged contact potential was also recorded. In order to detect mild-scuffing, instantaneous high speed friction was sampled at 10 kHz for 1 s every 60 s throughout the experiment. High speed contact potential measurements were recorded simultaneously.

The experiment was repeated but interrupted at the onset of mild-scuffing, based on the high speed friction values. Mild-scuffing was determined by the increased departure from the square wave at the reversal positions, approximately 100% greater than the mid-stroke.

Topographies of the scuffed cast iron wear scars were examined using a non-contact, focal plane variation microscope, Alicona Infinite Focus. Higher magnification images were obtained using a scanning electron microscope (SEM), Jeol 6500F at 20 kV, equipped with energy dispersive X-ray spectroscopy (EDX), Oxford instruments ISI with InCA software. To further investigate the material response to scuffing, a focused ion beam cross-section and microscopy images were taken perpendicular to the sliding direction to analyse the change in the subsurface micro-structure, using a Zeiss NVision 40 dual beam FIB.

## 3. Results

### 3.1. Materials

The roughness of the roller bearing samples, measured in the direction of reciprocation, had an  $R_a = 0.041 \pm 0.009$  μm. Surface grinding the cast iron flat plates achieved:  $R_a = 0.490 \pm 0.012$  μm,  $R_{pk} = 0.555 \pm 0.076$  μm,  $R_{vk} = 0.906 \pm 0.078$  μm and  $80 \pm 2\%$  plateau, Table 1. The lamellar graphite flakes, of the order of 100 μm,

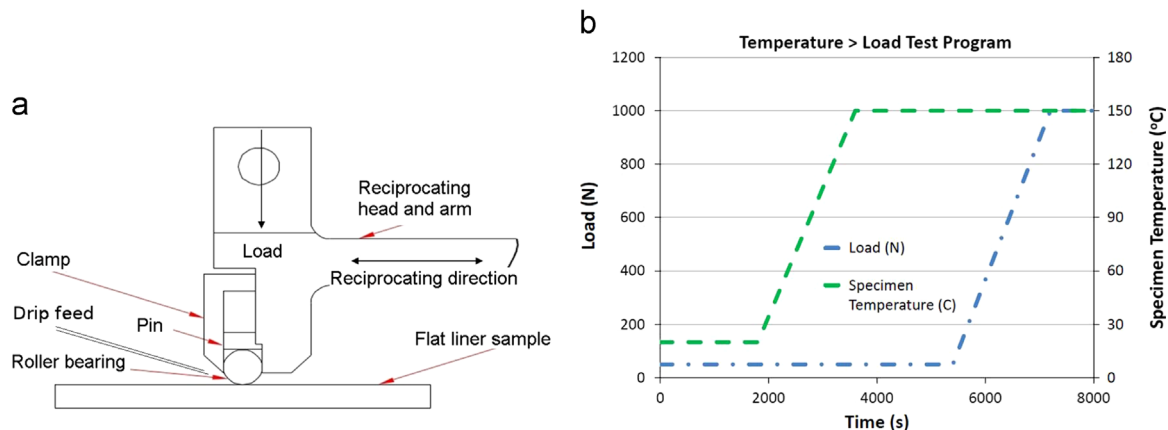


Fig. 1. TE-77: line contact configuration (a) and test program (b).

Download English Version:

<https://daneshyari.com/en/article/617131>

Download Persian Version:

<https://daneshyari.com/article/617131>

[Daneshyari.com](https://daneshyari.com)